ELSEVIER

Journal of Alloys and Compounds 457 (2008) 532–540

Journal of ALLOYS AND COMPOUNDS

www.elsevier.com/locate/jallcom

Synthesis, nuclear structure, and magnetic properties of $LaCr_{1-y}Mn_yO_3$ ($y = 0$, 0.1, 0.2, and 0.3)

M. Tseggai [a], P. Nordblad [a], R. Tellgren [b,*], H. Rundlöf [b], G. Andrè [c], F. Bourèe [c]

[a] *Department of Engineering Sciences, The Ångström Laboratory, Uppsala University, Box 534, SE-751 21 Uppsala, Sweden*
[b] *Department of Materials Chemistry, The Ångstrom Laboratory, Uppsala University, Box 538, SE-751 21 Uppsala, Sweden*
[c] *Laboratoire Lèon Brillouin, CEA-CNRS, Saclay, Gif sur Yvette F-91 191, France*

Received 14 January 2007; accepted 16 March 2007
Available online 23 March 2007

Abstract

The nuclear structure and magnetic properties of perovskite-type samples of compositions $LaCr_{1-y}Mn_yO_3$ ($y = 0$, 0.1, 0.2, 0.3) have been studied using neutron powder diffraction technique and magnetization measurements. All samples have orthorhombic structure with space group *Pnma* (No. 62) in the temperature range 1.5–400 K. The pure lanthanum chromate $LaCrO_3$ is a G-type antiferromagnet with a Néel temperature of 290 K. The Mn substituted samples also order antiferromagnetically at about 290 K, with canted magnetic moments yielding a ferromagnetic component.

Keywords: $LaCrO_3$; Manganese substitution; Neutron powder diffraction; Magnetic structure; Magnetic moment; Antiferromagnetism; SQUID

1. Introduction

Magnetic oxides of the perovskite-type structure have intriguing physical properties that are strongly dependent on doping with transition elements. Lanthanum chromate, $LaCrO_3$, is a perovskite-type material that has orthorhombic $GdFeO_3$-type structure at room temperature with space group, *Pbnm* (No. 62) [1,2] and lattice parmeters: $a = 5.477$ Å, $b = 5.514$ Å, and $c = 7.755$ Å [3]. $LaCrO_3$ undergoes an orthorhombic to rhombohedral structural transition at about 540 °C.

In the compound $LaCrO_3$, the Cr^{3+} ions have the same number of 3d electrons as the Mn^{4+} ions in $CaMnO_3$ [4]. It has also been reported that the magnetic structure of $LaCrO_3$ is identical to that of $CaMnO_3$ [5]. The magnetic ordering in $LaCrO_3$ is antiferromagnetic, G-type. In this type of ordering, the Cr^{3+} ion is antiferromagnetically coupled via the oxygen ions with all six nearest neighbours. A G-type antiferromagnetic magnetic structure persists also in the Mn-substituted compounds $LaCr_{1-y}Mn_yO_3$. Early reports on structural and magnetic properties of pure and doped lanthanum chromate can be found in Refs. [5–7].

This work deals with the synthesis and experimental investigations of the crystal structure and magnetic properties of $LaCr_{1-y}Mn_yO_3$ using X-ray and neutron powder diffraction technique together with magnetization measurements.

2. Experimental

Samples of nominal composition $LaCr_{1-y}Mn_yO_3$ ($y = 0.0$, 0.1, 0.2, and 0.3) were prepared by the standard solid-state reaction method. Before weighing the starting compounds, the La_2O_3 was heated in a furnace at 900 °C in an oxygen atmosphere for 15 h to drive out any moisture contained in the material. Stoichiometric amounts of La_2O_3, Cr_2O_3, and MnO were thoroughly mixed in ethanol and preheated in the furnace at 950 °C in air for 15 h. The powders were then taken out from the furnace and grounded in an agate mortar, pressed into tablets and heated in the furnace at 1100 °C in air for 48 h. The samples were then sintered at 1250 and 1300 °C in air for 48 and 52 h, respectively. The so prepared samples were crushed and thoroughly grounded to powder. The samples were checked for phase purity by a Guinier camera model V-FXC using Cu Kα radiation and Si as an internal standard, after sintering at 1250 °C and after sintering at 1300 °C. The samples were found to be single phased at both temperatures with an orthorhombic structure, space group *Pnma* (No. 62).

Neutron powder diffraction data were recorded at Studsvik, Sweden, by the neutron powder diffractometer with 35 ^{3}He detectors using a wavelength of $\lambda = 1.470(1)$ Å. Data was collected at 10, 295, 400, and 600 K over the angular range $4.0° \leq 2\theta \leq 139.92°$ with step size 0.08° in 2θ. For detailed studies of the magnetic properties of the samples, neutron powder diffraction data were also recorded at Laboratoire Léon Brillouin, CEA, Saclay, France, on the 2-axis powder diffractometer G 4-1 using a neutron wavelength of $\lambda = 2.43$ Å. The data

* Corresponding author: Tel.: +46 18 4713776; fax: +46 18 320355.
E-mail address: Roland.Tellgren@mkem.uu.se (R. Tellgren).

0925-8388/$ – see front matter © 2007 Elsevier B.V. All rights reserved.
doi:10.1016/j.jallcom.2007.03.069

Table 1
Structural parameters and reliability factors of $LaCr_{1-y}Mn_yO_3$ samples at 295 K

Atom	x	y	z	Biso	Occ
$LaCrO_3$ (a = 5.4743(3), b = 7.7543(7), c = 5.5118(5), Vol = 233.97(3))					
A(La)	0.0177(4)	0.25	0.9952(6)	0.45(3)	0.50
B(Cr)	0	0	0.5	0.14(5)	0.50
O1	0.4920(7)	0.25	0.0656(5)	0.49(2)	0.50
O2	0.2753(4)	0.0353(3)	0.7269(4)	0.49(2)	1.00
Reliability factors: R_p = 3.47%, R_{wp} = 4.68%, R_B = 3.10%, χ^2 = 3.04					
$LaCr_{0.8}Mn_{0.2}O_3$ (a = 5.4822(5), b = 7.7688(8), c = 5.5153(6), Vol = 234.89(4) Å^3)					
A(La)	0.0170(4)	0.25	0.9925(7)	0.40(3)	0.50
B:Cr—Mn	0, 0	0, 0	0.5, 0.5	0.15(7), 0.15(7)	0.40, 0.10
O1	0.4913(7)	0.25	0.0626(6)	0.53(2)	0.50
O2	0.2774(3)	0.0373(3)	0.7272(4)	0.53(2)	1.00
Reliability factors: R_p = 3.83%, R_{wp} = 4.93%, R_B = 3.61%, χ^2 = 2.77					
$LaCr_{0.9}Mn_{0.1}O_3$ (a = 5.4797(4), b = 7.7650(8), c = 5.5144(6), Vol = 234.63(4))					
A(La)	0.0171(4)	0.25	0.9917(6)	0.31(3)	0.5
B/Cr—Mn	0, 0	0, 0	0.5, 0.5	0.27(5), 0.27(5)	0.45, 0.05
O1	0.4903(7)	0.25	0.0635(6)	0.52(2)	0.5
O2	0.2762(4)	0.0368(3)	0.7271(4)	0.52(2)	0.5
Reliability factors: R_p = 4.01%, R_{wp} = 5.18%, R_B = 4.05%, χ^2 = 2.47					
$LaCr_{0.7}Mn_{0.3}O_3$ (a = 5.4848(6), b = 7.773(1), c = 5.517(7), Vol = 235.21(5) Å^3)					
B/Cr—Mn	0, 0	0, 0	0.5, 0.5	0.2(1), 0.2(1)	0.35, 0.15
O1	0.4903(8)	0.25	0.0609(7)	0.62(3)	0.5
O2	0.2780(4)	0.0380(3)	0.7282(5)	0.62(3)	0.5
Reliability factors: R_p = 4.33%, R_{wp} = 5.66%, R_B = 3.92%, χ^2 = 2.79					

were collected at several temperatures between 1.5 and 300 K over the angular range 17.0° ≤ 2θ ≤ 96.9° with step size 0.1° in 2θ. The neutron powder diffraction data were analyzed by the Rietveld method using the computer program FullProf [8].

The magnetization measurements were performed on a Quantum Design MPMS XL SQUID magnetometer. In these measurements, magnetization as a function of temperature was collected in the temperature range 5–325 K at an applied magnetic field of 20 Oe. Magnetization as a function of magnetic field was also measured in the range 0–50 kOe and a temperature of 5 K.

3. Results

3.1. Crystal structure

The Rietveld analyses of the neutron powder diffraction data at 295 K showed that all samples, $LaCr_{1-y}Mn_yO_3$ (y = 0.0, 0.1, 0.2, and 0.3) was single phased with an orthorhombic perovskite structure. The nuclear structure of both the unsubstituted and of the substituted samples remains orthorhombic with space group *Pnma* (No. 62) at all temperatures between 1.5 and 400 K. The nuclear structural parameters and reliability factors at 295 K for the different samples are shown in Table 1. Rietveld refinement of neutron data recorded at 600 K, however, showed that all the samples had passed a phase transition to a rhombohedral structure with space group $R\bar{3}c$ (No. 167), in agreement with earlier reported results [3]. The lattice parameters of the samples at 400 and 600 K are given in Table 2.

As there are no significant differences in the diffraction patterns and nuclear structure of the samples between 1.5 and 400 K, the Rietveld refinement plot at 295 K shown in Fig. 1 and the unit cell nuclear structure shown in Fig. 2 are typical to all the samples. The octahedral coordination of Cr/Mn is shown in Fig. 3. The occupancy for La^{3+} remains full throughout the whole substitution range, whereas the occupancy of Cr^{3+} decreases with increasing Mn substitution. The orthorhombic lattice parameters are related to the simple cubic perovskite lattice parameter (a_p) by $a \approx c \approx (\sqrt{2})a_p$, $b \approx 2a_p$. The lattice parameters monotonously increase (Table 2) with increasing Mn-substitution and accordingly, the unit cell volume also continuously increases with increasing y, for example, from 234.0 Å^3 for y = 0.0 to 235.2 Å^3 for y = 0.3.

Table 2
The lattice parameters of $LaCr_{1-y}Mn_yO_3$ at 400 and 600 K

Sample	Orthorhombic (at 400 K)			Rhombohedral (at 600 K)		
	a (Å)	b (Å)	c (Å)	a (Å)	b (Å)	c (Å)
$LaCrO_3$	5.4822(4)	7.7676(7)	5.5220(5)	5.5315(4)	5.5315(4)	13.363(1)
$LaCr_{0.9}Mn_{0.1}O_3$	5.4855(5)	7.775(1)	5.5210(6)	5.5314(6)	5.5314(6)	13.382(1)
$LaCr_{0.8}Mn_{0.2}O_3$	5.4891(5)	7.781(1)	5.5232(7)	5.5368(5)	5.5368(5)	13.385(1)
$LaCr_{0.7}Mn_{0.3}O_3$	5.4900(6)	7.782(1)	5.5245(8)	5.5378(6)	5.5378(6)	13.384(1)

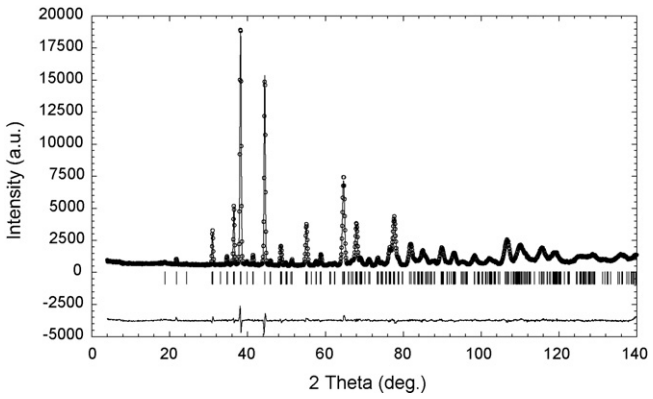

Fig. 1. Rietveld refinement plot of the neutron diffraction data for $LaCr_{0.8}Mn_{0.2}O_3$ sample at 295 K: the points are the observed intensity; the solid line is the calculated intensity; the short vertical lines are the positions of Bragg reflections; and the lower line is the difference between observed and calculated curves, $Y_{obs} - Y_{calc}$.

The oxidation state of Cr and Mn in all these compounds is nominally 3+ and the ionic radii of these ions (for 6-coordination) are: $R_{Mn}{}^{3+} = 0.65$ Å and $R_{Cr}{}^{3+} = 0.62$ Å. The Cr^{3+} and Mn^{3+} cations have 3 and 4 electrons in their 3d shells, respectively. Thus, the Mn^{3+}–Cr^{3+} electronic state is similar to that of the mixed valence state Mn^{3+}–Mn^{4+} in CMR manganites, and thus makes possible that ferromagnetic interaction of double exchange type may occur in the substituted samples. It can therefore be expected that Mn-substitution for Cr affects both the nuclear structure because ($R_{Mn}{}^{3+} > R_{Cr}{}^{3+}$) and magnetic properties (Mn^{3+}, Cr^{3+}) of the $LaCr_{1-y}Mn_yO_3$ system.

Apart from the slight increase of the cell volume that occurs with increasing Mn substitution, the nuclear structure is affected by a small change of the octahedral distortion (cf. Figs. 2 and 3) given by the O–O distances (Table 3). The O1–O1 distances essentially do not change with increasing Mn substitution, whereas the O2′–O2′ distances are somewhat elongated and O2–O2 distances slightly shortened with increasing Mn substitution. The O1–Cr/Mn–O2 and O1–Cr/Mn–O2′ bond angles at 295 K are given in Table 4 together with the tilt angle Cr/Mn–O1–Cr/Mn. As can be seen, the bond angles are not systematically altered by the substitution. Also the tilting of the octahedra, defined by Cr/Mn–O1–Cr/Mn bond angle, remains essentially unchanged at about 160° with increasing Mn substitution.

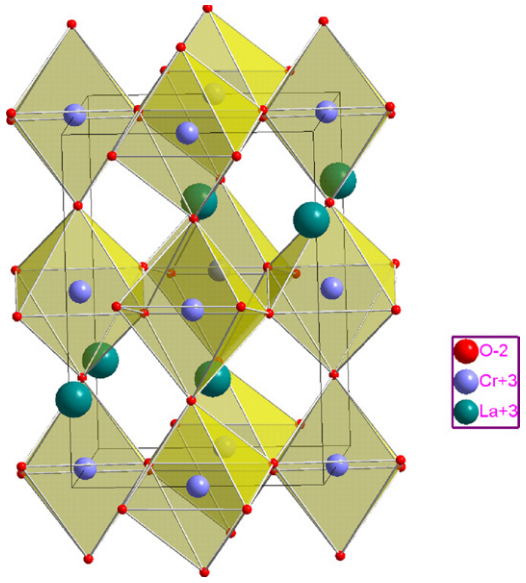

Fig. 2. The nuclear unit cell structure for $LaCrO_3$ at 295 K.

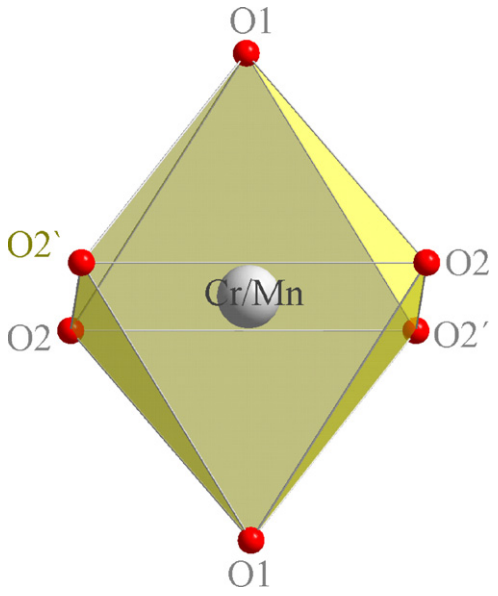

Fig. 3. The octahedral coordination in $LaCr_{1-x}Mn_xO_3$.

Table 3
O–O distances as a function of y

Mn-substitution	Bond length in Å at 295 K		
y	O1–O1	O2–O2	O2′–O2′
0.0	3.944(1)	3.930(2)	3.952(2)
0.1	3.947(1)	3.924(3)	3.970(3)
0.2	3.946(1)	3.917(3)	3.983(3)
0.3	3.946(1)	3.908(4)	3.999(4)

Cf. Figs. 2 and 3.

The octahedral distortion can be systematically quantified from the measured bond length distortion, Δ_S, and bond angle variance, δ, introduced by Shannon [9]:

$$\Delta_S = \frac{1}{6}\sum \frac{(r_i - r)^2}{r^2} \times 10^3, \quad (1)$$

Table 4
Dependence of O–Cr/Mn–O and Cr/Mn–O1–Cr/Mn bond angles as on y at 400 K

Mn substitution	Bond angles (°)		
y	O1–Cr/Mn–O2′	O1–Cr/Mn–O2	Cr/Mn–O–Cr/Mn
0.0	90.8(1)	88.6(1)	159.84(2)
0.1	91.1(2)	88.2(2)	160.33(3)
0.2	90.6(2)	88.7(2)	159.42(3)
0.3	90.9(2)	88.4(2)	159.87(4)

$$\delta = \sum \left\{ \frac{(\theta_i - 90)^2}{n-1} \right\}, \quad (2)$$

where r_i and r are the individual and average bond lengths, respectively, and θ_i are individual O–B–O bond angles. Applying (1) and (2) to our $LaCr_{1-y}Mn_yO_3$ series of samples, we find that Δ_B is 0.0145 and 0.0753 and δ is 1.77 and 2.07 for $y = 0.0$ and 0.3, respectively. Although significantly increased with increasing Mn substitution, the calculated Δ_B and δ values can be considered as minor distortions, and therefore, the octahedral distortions do not cause structural changes in the compounds. The nuclear structure of the $LaCr_{1-y}Mn_yO_3$ system remains orthorhombic with space group *Pnma* (No. 62) in the whole range of Mn substitution ($0.0 \leq y \leq 0.3$) and also in the temperature range between 1.5 and 400 K.

3.2. Magnetic properties

The temperature dependence of the magnetization of the four samples at a weak applied field is shown in Fig. 4a–d. The measurements have been made by cooling the samples to 5 K in zero applied magnetic field, apply the magnetic field (20 Oe) at this temperature and measure the magnetization while heating the sample to 325 K (zero field cooled (ZFC) magnetization). The field is kept constant and the magnetization again recorded on cooling the sample back to 5 K (field cooled (FC) magnetization). The temperature dependence of the magnetization clearly reveals an antiferromagnetic transition temperature at about 290 K in all samples. The transition occurs at the temperature where the ZFC and FC curves split and the ZFC magnetization shows a sharp maximum. For the $y = 0$ compound this transition is the most significant observation. For the doped samples, the antiferromagnetic transition is seen as a weak anomaly at about 290 K (see insets of Fig. 4b–d). There are however, striking additional features at lower temperatures as is seen in the main frames of the figures. A dramatic increase of the magnetization occurs that indicates the appearance of a significant uncompensated spontaneous moment in the samples of increasing magnitude with increasing Mn content. (Compare the magnitude of the signal for the different samples and in the insets.) A large irreversibility between the FC and ZFC magnetization also appears

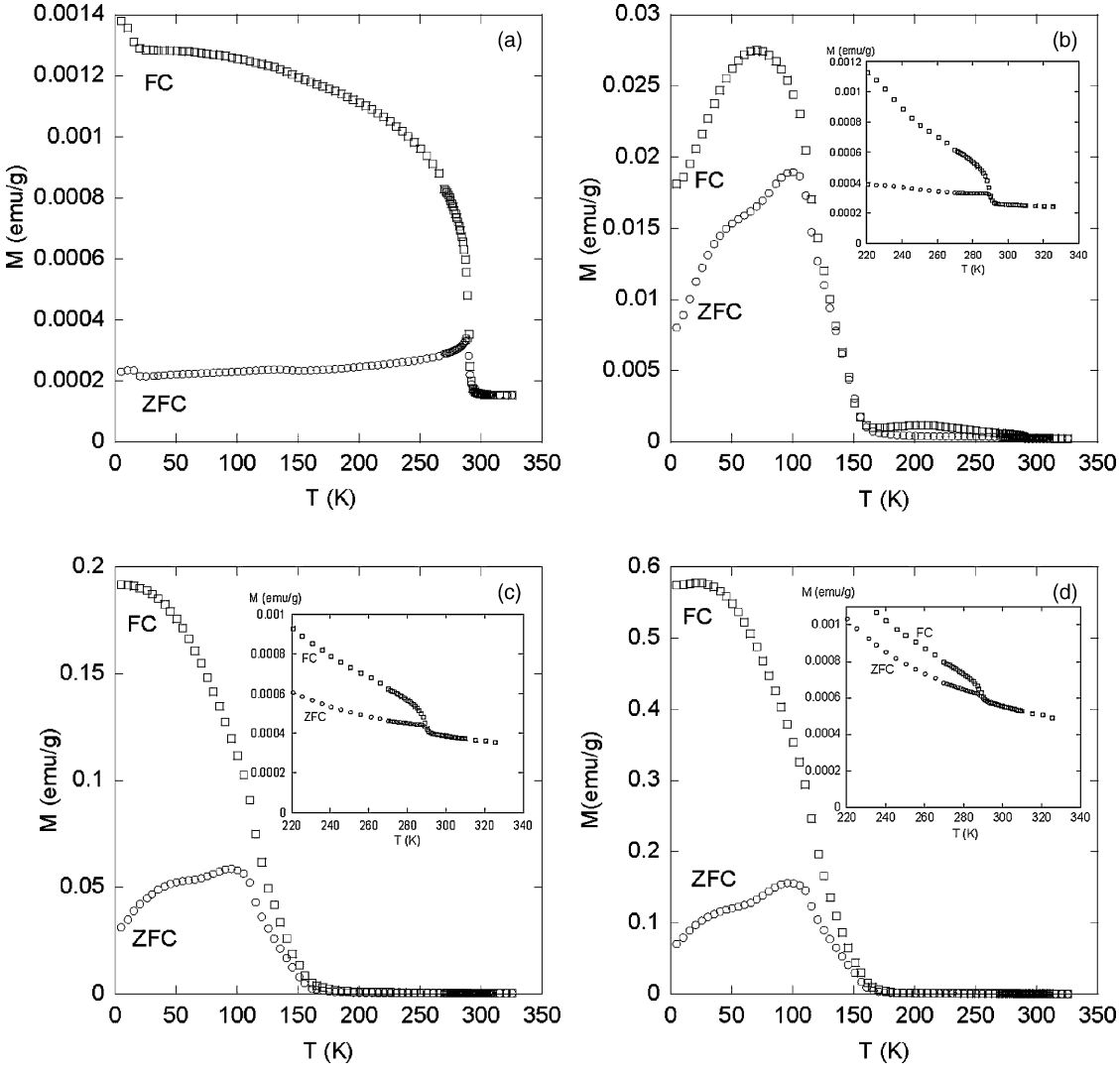

Fig. 4. The dependence of magnetization on temperature for (a) $LaCrO_3$, (b) $LaCr_{0.9}Mn_{0.1}O_3$, (c) $LaCr_{0.8}Mn_{0.2}O_3$, and (d) $LaCr_{0.7}Mn_{0.3}O_3$. $H = 200$ Oe.

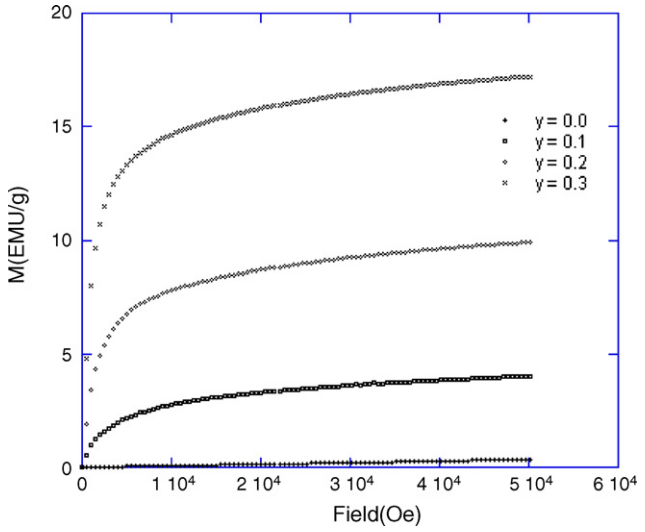

Fig. 5. Magnetization as a function of applied field at 5 K for $LaCr_{1-y}Mn_yO_3$.

at the temperature of the rapid increase of the magnetization (slightly above 150 K in all three samples). Fig. 5 shows magnetization versus field curves measured at 5 K in fields varying from 0 to 50 kOe. The curves show that the pure sample shows a 'paramagnetic' response, i.e. a linear increase of the magnetization with field characteristic of a pure antiferromagntic phase. The three doped samples shows that a spontaneous excess magnetization of increasing size is superposed on the antiferromagnetic response. The magnitude of this moment increases from about 3 emu/g for the $y = 0.1$ sample to 8 emu/g for $y = 0.2$ and reaches about 15 emu/g for the $y = 0.3$ sample. Fig. 6a and b shows full hysteresis curves for the $y = 0$ and the $y = 0.2$ samples. It can be noted from this figure that some deviation from a linear response is seen for the $y = 0$ sample, that corresponds to alignment of the weak excess magnetization that is clearly seen in difference between the ZFC and FC curves in Fig. 4a. The $y = 0.2$ sample shows a hysteresis curve with very small and on this scale barely resolved coercivity.

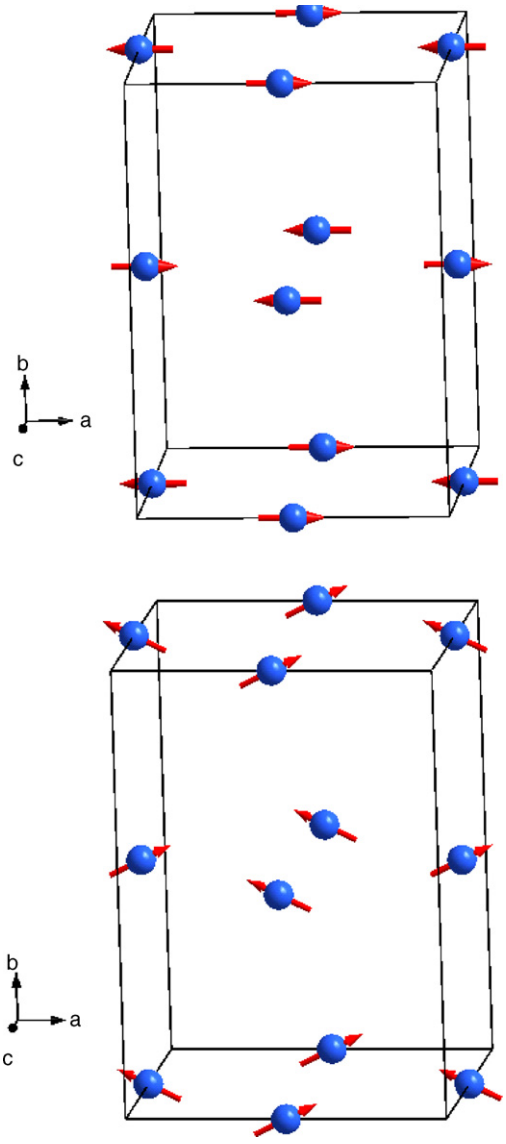

Fig. 7. The magnetic structure at 1.5 K for (a) $LaCrO_3$ and (b) $LaCr_{0.8}Mn_{0.2}O_3$.

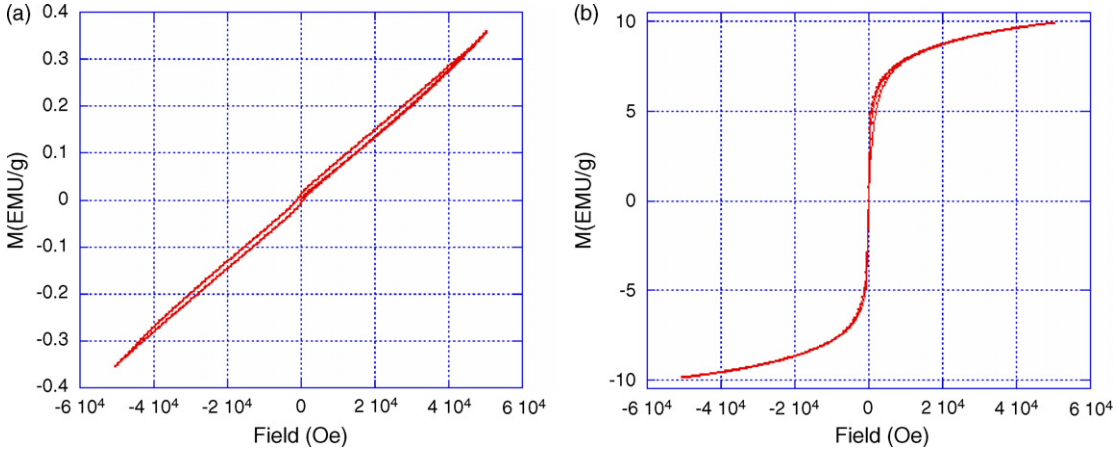

Fig. 6. Hysteresis curves at 5 K for (a) $LaCrO_3$ and (b) $LaCr_{0.8}Mn_{0.2}O_3$.

3.3. Magnetic structure

A detailed study of the magnetic structure was made from the Rietveld refinement of the neutron powder data collected on the 2-axis powder diffractometer G 4-1 at Saclay. In the refinements the values of occupancies obtained from the refinement of the neutron powder data recorded at 295 K on the high resolution neutron powder diffractometer in Studsvik, were used. The neutron scattering lengths of the different elements are: La = 8.240, Cr = 3.635, Mn = −3.73 and O = 5.803 fm. The magnetic form factors are those from the FullProf program. The total number of reflexions generated is 69. The values of the thermal parameters, which are difficult to refine when only low angle data are available, have been fixed at their 10 and 295 K values, obtained by Rietveld refinement of the neutron data recorded at 10 and 295 K in Studsvik. The values of the thermal parameters at 10 K were used in the refinements for all temperatures between 1.5 and 150 K and their room temperature values were used for all temperatures in the range 150–300 K.

The parent compound $LaCrO_3$ is antiferromagnetic of the G-type structure (Fig. 7a) with a strong intensity on the 10-1 reflexion but no intensity at all on the 0-11 reflexion (Fig. 8a, $y = 0.0$). With increasing Mn substitution the intensity of the 10-1 reflexion is reduced while the intensity on the 0-11 reflexion increases (Fig. 8a). Our interpretation of the changes in intensity of these two reflexions is a canting of the magnetic moments giving a ferromagnetic component in the *b*-direction (Fig. 7b).

Fig. 8b shows the intensities for $LaCr_{0.8}Mn_{0.2}O_3$ at different temperatures from which is clearly seen that the antiferromagnetic contribution diminishes with increasing temperature and at about 300 K, essentially vanishes. A small ferromagnetic moment on the other hand still exists.

The final refinement plots based on the data obtained from the powder diffractometer G4.1 in Saclay is shown in Fig. 9a and b for $LaCrO_3$ and $LaCr_{0.8}Mn_{0.2}O_3$, respectively at 1.5 K. The refined nuclear and magnetic structural parameters as well as the values of the magnetic moments at some temperatures and the corresponding reliability factors R_p, R_{wp}, R_B, and R_M are given in Table 5 .

The derived magnitudes of the magnetic moments obtained from the Rietveld refinements on the Cr/Mn site at all measured temperatures are plotted versus temperature in Fig. 10. The antiferromagnetic moment decreases with increasing temperature and disappears at about 290 K for all samples, in good agreement with the result derived from the magnetization measurements. It is also seen that the magnitude of the AF moment continuously decrease with increasing Mn doping, for example, at 1.5 K from 2.6 μ_B/Cr/Mn for $y = 0$ to 2.0 μ_B/Cr/Mn for $y = 0.3$.

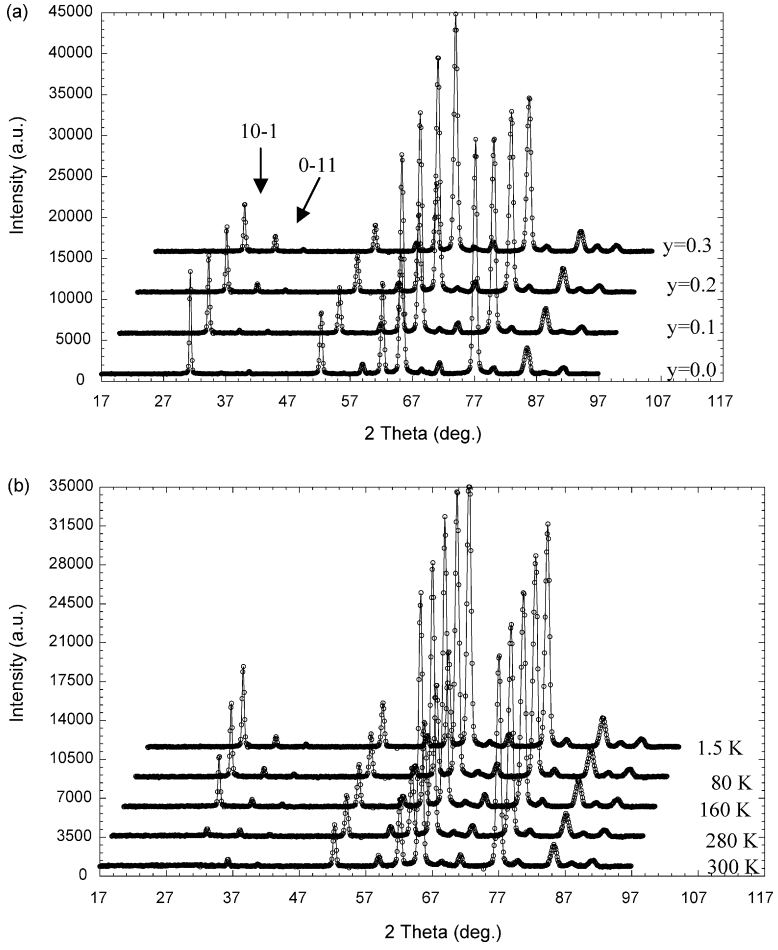

Fig. 8. Observed intensities of the neutron diffraction data. (a) At 1.5 K for the different compositions and (b) for the $LaCr_{0.8}Mn_{0.2}O_3$ sample at different temperatures. The plots are shifted with respect to both the intensity and the 2θ axis.

Table 5
Structural and magnetic parameters for the samples at some temperatures as determined by Rietveld refinement: in the magnetic structure (MS) column, G and F represent G-type antiferromagnetic and ferromagnetic structures, respectively

Atom	x	y	z	BISO	OCC	T (K)	MS	M_x (μ_B)	M_y (μ_B)	M_z (μ_B)	M (μ_B)
$LaCr_{1-y}Mn_yO_3$, $y = 0.0$											
La	0.0212(7)	0.25	0.996(2)	0.14(3)	0.50	1.5					
Cr	0	0	0.50	0.01(5)	0.50		G	2.63(3)			2.63(3)
O1	0.492(1)	0.25	0.062(2)	0.24(3)	0.50						
O2	0.275(1)	0.0356(8)	0.726(1)	0.24(3)	1.00						
$a = 5.5027(3)$ Å, $b = 7.7979(9)$ Å, $c = 5.5347(4)$ Å; $R_p = 4.56\%$, $R_{wp} = 6.24\%$, $R_B = 2.12\%$, $R_M = 1.47\%$											
La	0.0200(7)	0.25	0.997(2)	0.14(3)	0.50	150					
Cr	0	0	0.50	0.01(5)	0.50		G	2.38(3)			2.38(3)
O1	0.491(1)	0.25	0.062(2)	0.24(3)	0.50						
O2	0.274(1)	0.0353(8)	0.727(1)	0.24(3)	1.00						
$a = 5.5028(3)$ Å, $b = 7.799(1)$ Å, $c = 5.5362(4)$ Å; $R_p = 4.77\%$, $R_{wp} = 6.42\%$, $R_B = 2.13\%$, $R_M = 2.21\%$											
La	0.0178(9)	0.25	0.997(2)	0.44(3)	0.50	295					
Cr	0	0	0.50	0.12(4)	0.50		G	0			0
O1	0.492(1)	0.25	0.059(2)	0.46(3)	0.50						
O2	0.274(1)	0.0374(9)	0.727(1)	0.46(2)	1.00						
$a = 5.5081(4)$ Å, $b = 7.808(1)$ Å, $c = 5.5430(4)$ Å, $R_p = 5.33\%$, $R_{wp} = 7.09\%$, $R_B = 3.85\%$											
$LaCr_{1-y}Mn_yO_3$, $y = 0.1$											
La	0.0214(6)	0.25	0.997(1)	0.18(3)	0.50	1.5					
Cr	0	0	0.50	0.10(5)	0.45		G/F	2.52(3)/0	0/0.56(5)	–	2.57(3)
Mn	0	0	0.50	0.10(5)	0.05						
O1	0.4907(9)	0.25	0.062(2)	0.33(2)	0.50						
O2	0.2768(8)	0.0358(7)	0.7270(9)	0.33(2)	1.00						
$a = 5.5002(3)$ Å, $b = 7.7919(8)$ Å, $c = 5.5315(3)$ Å; $R_p = 3.61\%$, $R_{wp} = 5.05\%$, $R_B = 1.85\%$, $R_M = 1.65\%$											
La	0.0201(8)	0.25	0.996(2)	0.18(3)	0.50	150					
Cr	0	0	0.50	0.10(5)	0.45		G/F	2.19(3)/0	0/0.49(6)	–	2.24(3)
Mn	0	0	0.50	0.10(5)	0.05						
O1	0.491(1)	0.25	0.063(2)	0.33(2)	0.50						
O2	0.2758(9)	0.0356(7)	0.727(1)	0.33(2)	1.00						
$a = 5.5017(3)$ Å, $b = 7.7943(8)$ Å, $c = 5.5336(4)$ Å; $R_p = 3.95\%$, $R_{wp} = 5.37\%$, $R_B = 1.74\%$, $R_M = 2.24\%$											
La	0.0191(8)	0.25	0.997(1)	0.31(3)	0.50	295					
Cr	0	0	0.50	0.27(5)	0.45		G/F	0	0	–	0
Mn	0	0	0.50	0.27(5)	0.05						
O1	0.492(1)	0.25	0.063(2)	0.52(2)	0.50						
O2	0.276(1)	0.0369(8)	0.728(1)	0.52(2)	1.00						
$a = 5.5069(4)$ Å, $b = 7.804(1)$ Å, $c = 5.5413(4)$ Å; $R_p = 4.47\%$, $R_{wp} = 5.95\%$, $R_B = 3.01\%$,											
$LaCr_{1-y}Mn_yO_3$, $y = 0.2$											
La	0.0219(6)	0.25	0.997(1)	0.21(3)	0.50	1.5					
Cr	0	0	0.50	0.14(7)	0.40		G/F	2.27(2)/0	0/0.83(4)	–	2.41(2)
Mn	0	0	0.50	0.14(7)	0.10						
O1	0.491(1)	0.25	0.064(2)	0.38(2)	0.50						
O2	0.2780(9)	0.0359(7)	0.728(1)	0.38(2)	1.00						
$a = 5.5038(3)$ Å, $b = 7.7931(7)$ Å, $c = 5.5339(4)$ Å; $R_p = 3.78\%$, $R_{wp} = 5.32\%$, $R_B = 2.09\%$, $R_M = 1.76\%$											
La	0.0213(7)	0.25	0.996(1)	0.21(3)	0.50	150					
Cr	0	0	0.50	0.14(7)	0.40		G/F	1.86(2)/0	0/0.55(6)	–	1.94(3)
Mn	0	0	0.50	0.14(7)	0.10						
O1	0.491(1)	0.25	0.065(2)	0.38(2)	0.50						
O2	0.2776(9)	0.0348(8)	0.727(1)	0.38(2)	1.00						
$a = 5.5062(4)$ Å, $b = 7.7971(8)$ Å, $c = 5.5368(4)$ Å; $R_p = 4.06\%$, $R_{wp} = 5.58\%$, $R_B = 2.16\%$, $R_M = 3.06\%$											
La	0.0193(7)	0.25	0.996(1)	0.42(3)	0.50	295					
Cr	0	0	0.50	0.15(6)	0.40		G/F	0	0/0.53(5)	–	0.53(5)
Mn	0	0	0.50	0.15(6)	0.10						
O1	0.491(1)	0.25	0.066(1)	0.53(2)	0.50						
O2	0.2765(7)	0.0348(7)	0.729(1)	0.53(2)	1.00						

Table 5 (*continued*)

Atom	*x*	*y*	*z*	BISO	OCC	*T* (K)	MS	M_x (μ_B)	M_y (μ_B)	M_z (μ_B)	*M* (μ_B)
$a = 5.5101(4)$ Å, $b = 7.8048(9)$ Å, $c = 5.5435(4)$ Å; $R_p = 4.06\%$, $R_{wp} = 5.62\%$, $R_B = 2.13\%$, $R_M = 5.59\%$											
$LaCr_{1-y}Mn_yO_3$, $y = 0.3$											
La	0.0223(6)	0.25	0.998(1)	0.21(4)	0.50	1.5					
Cr	0	0	0.50	0.1(1)	0.35		G/F	2.03(2)/0	0/1.13(4)	–	2.32(3)
Mn	0	0	0.50	0.1(1)	0.15						
O1	0.490(1)	0.25	0.069(2)	0.46(3)	0.50						
O2	0.2786(9)	0.0339(7)	0.729(1)	0.46(3)	1.00						
$a = 5.5048(4)$ Å, $b = 7.791(1)$ Å, $c = 5.5346(5)$ Å; $R_p = 3.97\%$, $R_{wp} = 5.67\%$, $R_B = 2.06\%$, $R_M = 3.39\%$											
La	0.0209(7)	0.25	0.999(2)	0.21(4)	0.50	150					
Cr	0	0	0.50	0.1(1)	0.35		G/F	1.57(2)/0	0/0.55(7)	–	1.66(3)
Mn	0	0	0.50	0.1(1)	0.15						
O1	0.490(1)	0.25	0.068(2)	0.46(3)	0.50						
O2	0.2788(9)	0.0344(8)	0.729(1)	0.46(3)	1.00						
$a = 5.5061(4)$ Å, $b = 7.794(1)$ Å, $c = 5.5365(5)$ Å; $R_p = 4.14\%$, $R_{wp} = 5.86\%$, $R_B = 2.16\%$, $R_M = 4.89\%$											
La	0.0189(7)	0.25	0.998(1)	0.39(3)	0.50	295					
Cr	0	0	0.50	0.2(1)	0.35		G/F	0	0/0.47(7)	–	0.47(7)
Mn	0	0	0.50	0.2(1)	0.15						
O1	0.489(1)	0.25	0.065(2)	0.62(3)	0.50						
O2	0.2780(9)	0.0360(7)	0.730(1)	0.62(3)	1.00						
$a = 5.5101(4)$ Å, $b = 7.804(1)$ Å, $c = 5.5434(5)$ Å; $R_p = 3.90\%$, $R_{wp} = 5.50\%$, $R_B = 2.20\%$, $R_M = 11.6\%$											

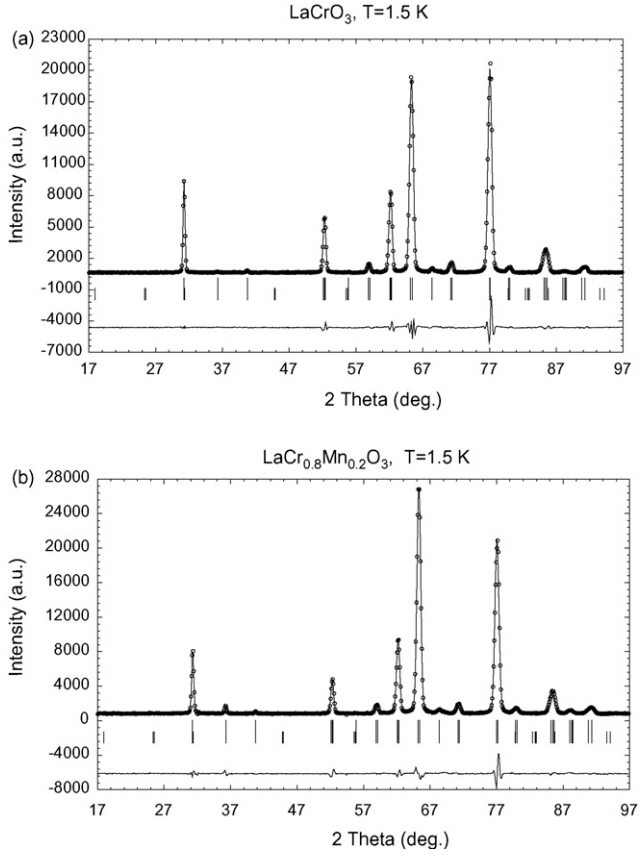

Fig. 9. Rietveld refinement plots at 1.5 K for (a) $LaCrO_3$ and (b) $LaCr_{0.8}Mn_{0.2}O_3$. The points are the observed intensity; the solid line is the calculated intensity; the short upper vertical lines are the positions of the nuclear Bragg reflections and the lower the magnetic.

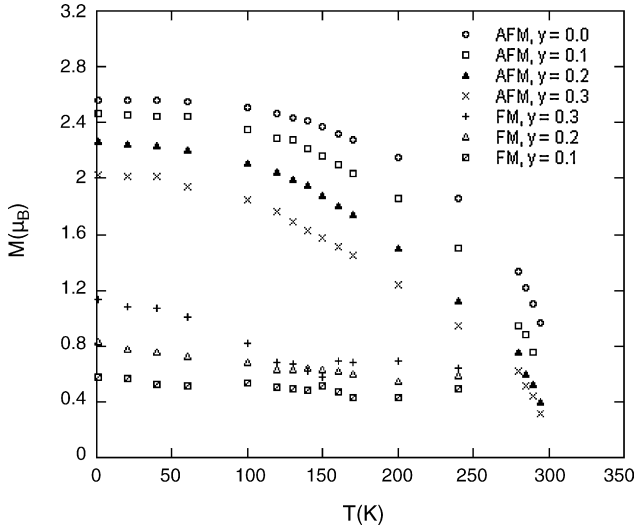

Fig. 10. Dependence of magnetic moment on temperature for $LaCr_{1-y}Mn_yO_3$ derived from the Rietveld refinement of the neutron powder diffraction data recorded in the temperature range 1.5–300 K.

The derived ferromagnetic component of the magnetic moment for the different samples is also plotted in Fig. 10. As can be seen, a small ferromagnetic moment still exists at 300 K, which also could be observed in Fig. 8b.

4. Discussion and conclusions

The nuclear structure of $LaCr_{1-y}Mn_yO_3$ does not change from the original structure of $LaCrO_3$ when Cr is replaced by Mn to concentrations up to $y = 0.3$. Such a stability of the original structure to substitution is common in perovskite oxides that crystallize in the orthorhombic *Pnma* (No. 62) structure.

The antiferromagnetic transition is in all samples accompanied by the appearance of a weak spontaneous excess magnetization that aligns with a weak applied magnetic field and causes a large difference between the low field zero field cooled and the field cooled magnetization curves. Such an excess magnetization is expected to arise in systems with mixed magnetic ions like the current doped samples, but is more surprising but not unique for the pure antiferromagnet $LaCrO_3$.

The magnetic properties are on the other hand quite dramatically and in some aspects surprisingly affected by the substitution. The origin of the rather strong influence may be found in the fact that the replacement of Cr^{3+} by Mn^{3+} not only alters the magnitude of the magnetic moment on the B site, but also possibly introduce ferromagnetic double exchange interaction that brings competing ferro- and antiferromagnetic interaction to the system. This additional interaction is responsible for the observed canting of the magnetic moments in the doped samples. It is on the other hand quite remarkable that the antiferromagnetic transition temperature remains at 290 K essentially unchanged by substitution. The occurrence of a maximum in the FC curve of the $y = 0.1$ sample is an indication that a re-entrant spin glass phase is entered at low temperatures. The re-entrance is possibly caused by the existence of both ferro- and antiferromagnetic interactions and a random distribution of the two magnetic ions.

Acknowledgements

Financial support from Sida/SAREC to the Asmara Program at Uppsala University and the support from the Swedish Research Council (VR) are gratefully acknowledged.

References

[1] S. Geller, J. Chem. Phys. 24 (1956) 1236.
[2] S. Geller, Acta Crystallogr. 10 (1957) 243.
[3] S. Geller, P.M. Raccah, Phys. Rev. B 2 (1970) 1167.
[4] W.C. Koehler, E.O. Wollan, J. Phys. Chem. Solids 2 (1957) 100.
[5] U.H. Bents, Phys. Rev. 106 (1957) 225.
[6] J.B. Goodenough, Magnetism and the Chemical Bond, Interscience Publishers, New York/London, 1963, p. 100.
[7] T. Arakawa, S. Tsuchi-ya, J. Shiokawa, Mater. Res. Bull. 16 (1981) 97.
[8] J. Rodriguez-Carvajal, Physica B 192 (1993) 55.
[9] R.D. Shannon, Acta Cryst. A 32 (1976) 751.